

Simulations of vibrated granular medium with impact-velocity-dependent restitution coefficientSean McNamara^{1,*} and Eric Falcon^{2,†}¹*Centre Européen de Calcul Atomique et Moléculaire, 46, allée d'Italie, 69 007 Lyon, France*²*Laboratoire de Physique, École Normale Supérieure de Lyon, UMR 5672, 46, allée d'Italie, 69 007 Lyon, France*

(Received 30 November 2004; published 24 March 2005)

We report numerical simulations of strongly vibrated granular materials designed to mimic recent experiments performed in both the presence and the absence of gravity. The coefficient of restitution used here depends on the impact velocity by taking into account both the viscoelastic and plastic deformations of particles, occurring at low and high velocities, respectively. We show that this model with impact-velocity-dependent restitution coefficient reproduces results that agree with experiments. We measure the scaling exponents of the granular temperature, collision frequency, impulse, and pressure with the vibrating piston velocity as the particle number increases. As the system changes from a homogeneous gas state at low density to a clustered state at high density, these exponents are all found to decrease continuously with increasing particle number. All these results differ significantly from classical inelastic hard sphere kinetic theory and previous simulations, both based on a constant restitution coefficient.

DOI: 10.1103/PhysRevE.71.031302

PACS number(s): 45.70.-n, 05.20.Dd, 05.45.Jn

I. INTRODUCTION

The past decade has seen the publication of many experimental [1–3], numerical [3–5], and theoretical [1,6–8] studies of strongly vibrated granular media. This problem is interesting because vibrated granular media are simple but nontrivial examples of nonequilibrium steady states and the only way to experimentally realize granular gases [9]. However, numerous questions remain about the link between experiments on one hand, and theory and simulations on the other. Most numerical and theoretical studies were not intended to be compared with experiments. Therefore, they have parameter values far from the experimental ones, and none of them predict even the most basic features of the experimental results.

In this paper, we bridge the gap between experiments and numerics by presenting simulations of strongly vibrated granular materials designed to mimic recent experiments performed in both the presence [10] and the absence [11] of gravity. We present simulations that resemble the experiments for a large range of parameters. We show that two parameters are especially important for the agreement between experiment and simulation. First of all, the coefficient of restitution has to be dependent on the particle impact velocity by taking into account both the viscoelastic and plastic deformations of particles occurring at low and high velocities, respectively. Most previous numerical studies consider only a constant restitution coefficient [3–5]; a few studies with slight velocity dependence (due to only the viscoelastic contribution) [12]. Second, it is important to explicitly consider the number of particles N . Studying only one value of N or comparing results obtained at different N can lead to interpretive difficulties.

Beyond these agreements between experiments and our simulations, we find results that differ significantly from classical inelastic hard sphere kinetic theory and previous simulations. We measure the scaling exponents of the granular temperature, collision frequency, impulse, and pressure with the vibrating piston velocity as the particle number increases, in both the presence and absence of gravity. We show that the system undergoes a smooth transition from a homogeneous gas state at low density to a clustered state at high density.

The paper has the following structure. In Sec. II, we present a description of the simulations (notably the model of impact-velocity-dependent restitution coefficient, and the influence of other simulations parameters). Section III provides a comparison of simulations and experiments (showing the importance of the variable coefficient of restitution and the particle number), and the results of the scaling exponents. Section III C focus on the influence of other simulations parameters (bed height, box size, particle rotations, gravity). Finally, in Sec. IV we summarize our results.

II. DESCRIPTION OF THE SIMULATIONS**A. The variable coefficient of restitution**

The greatest difference between our simulations and the previous numerical studies of vibrated granular media [3–5] is that we use a restitution coefficient that depends on impact velocity. The restitution coefficient r is the ratio between the relative normal velocities before and after impact. In previous simulations of strongly vibrated granular media, the coefficient of restitution is considered to be constant and lower than 1. However, for a century, it has been shown from impact experiments that r is a function of the impact velocity v [13–17]. Indeed, for metallic particles, when v is large ($v \geq 5$ m/s [14]), the colliding particles deform fully plastically and $r \propto v^{-1/4}$ [13–15]. When $v \leq 0.1$ m/s [14], the deformations are elastic with mainly viscoelastic dissipation, and $(1-r) \propto v^{1/5}$ [15–18]. Such velocity-dependent restitution

*Permanent address: I.C.P., Universität Stuttgart, 70569 Stuttgart, Germany.

†Email address: Eric.Falcon@ens-lyon.fr;

URL: <http://perso.ens-lyon.fr/eric.falcon/>

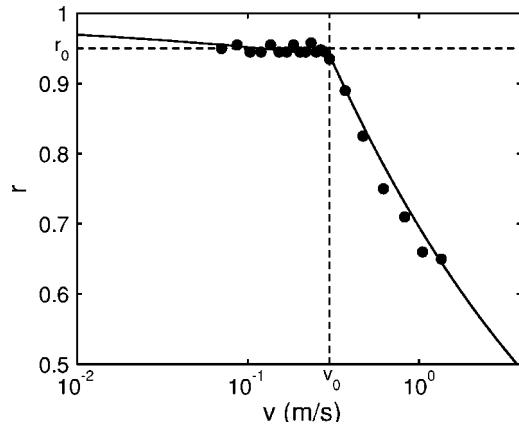


FIG. 1. The restitution coefficient r as a function of impact velocity v , as given in Eq. (1) (solid line). The dashed lines show $v_0=0.3$ m/s and $r_0=0.95$. Experimental points (●) for steel spheres were extracted from Fig. 1 of Ref. [25].

coefficient models have recently been shown to be important in numerical [12,19–23] and experimental [17,24] studies. Applications include granular fluidlike properties (convection [19], surface waves [20]), collective collisional processes (energy transmission [21], absence of collapse [17,22]), and planetary rings [23,24]. But surprisingly, this model has not apparently yet been tested numerically for strongly vibrated granular media.

In this paper, we use a velocity-dependent restitution coefficient $r(v)$ and join the two regimes of dissipation (viscoelastic and plastic) together as simply as possible, assuming that

$$r(v) = \begin{cases} 1 - (1 - r_0) \left(\frac{v}{v_0} \right)^{1/5}, & v \leq v_0, \\ r_0 \left(\frac{v}{v_0} \right)^{-1/4}, & v \geq v_0, \end{cases} \quad (1)$$

where $v_0=0.3$ m/s is chosen, throughout the paper, to be the yielding velocity for stainless steel particles [14,25] for which r_0 is close to 0.95 [25]. Note that $v_0 \sim 1/\sqrt{\rho}$ where ρ is the density of the sphere [14]. We display in Fig. 1 the velocity-dependent restitution coefficient of Eq. (1), with $r_0=0.95$ and $v_0=0.3$ m/s, which agrees well with experimental results on steel spheres from Ref. [25]. As also already noted by Ref. [14], the impact velocity to cause yield in metal surfaces is indeed relatively small. For metal, it mainly comes from the low yield stress value ($Y \sim 10^9$ N/m²) with respect to the elastic Young modulus ($E \sim 10^{11}$ N/m²). Most impacts between metallic bodies thus involve some plastic deformation.

B. The other simulation parameters

The numerical simulation consists of an ensemble of identical hard disks of mass $m \approx 3 \times 10^{-5}$ kg excited vertically by a piston in a two-dimensional box. Simulations are done both in the presence ($g=9.8$ m/s²) and absence ($g=0$) of uniform gravity g . Collisions are assumed instantaneous and thus

only binary collisions occur. For simplicity, we neglect the rotational degree of freedom. Collisions with the wall are treated in the same way as collisions between particles, except the wall has infinite mass.

Motivated by recent three-dimensional (3D) experiments on stainless steel spheres, 2 mm in diameter, fluidized by a vibrating piston [10], we choose the simulation parameters to match the experimental ones: in the simulations, the vibrated piston at the bottom of the box has amplitude $A=25$ mm (distance between the highest and lowest positions of the piston) and frequencies $5 \leq f \leq 50$ Hz. The piston is nearly sinusoidally vibrated with a wave form made by joining two parabolas together. The vertical displacement of the piston $z(t)$ during time t then is $z(t)=(A/2)(t^2-t_0^2)$ for $-t_0 \leq t \leq t_0$ and $z(t)=-(A/2)(t^2-t_0^2)$ for $t_0 \leq t \leq 3t_0$ with $t_0=1/(4f)$. This leads to a maximum piston velocity given by $V=4Af$. The particles are disks $d=2$ mm in diameter with stainless steel collision properties through v_0 and r_0 (see Fig. 1). The box has width $L=20$ cm and horizontal periodic boundary conditions. Since our simulations are two dimensional, we consider the simulation geometrically equivalent to the experiment when their numbers of layers of particles, $n=Nd/L$, are equal. Hence in the simulation, a layer of particles $n=1$ corresponds to 100 particles. We checked that n is an appropriate way to measure the number of particles by also running simulations at $L=10$ and 40 cm. None of this paper's results depend significantly on L . As in the experiments, the height h of the box depends on the number of particles in order to have a constant difference $h-h_0=15$ mm, where h_0 is the height of the bed of particles at rest. Heights are defined from the piston at its highest position. The influence of $h-h_0$ on the results is discussed in Sec. III C.

III. COMPARISON OF SIMULATION AND EXPERIMENT: SCALING PROPERTIES

A. The importance of the variable coefficient of restitution

We examine first the dependence of the pressure on the number of particle layers for maximum velocity of the piston $1 \leq V \leq 5$ m/s ($V=4Af$). The time averaged pressure at the upper wall is displayed in Fig. 2 as a function of n for various f : from the experiments of Falcon *et al.* [10] [see Fig. 2(a)], from our simulations with velocity-dependent restitution coefficient $r=r(v)$ proposed in Eq. (1) [see Fig. 2(b)], with constant restitution coefficient $r=0.95$, often used to describe steel particles [see Fig. 2(c)], and finally with an unrealistic constant restitution coefficient $r=0.7$ [see Fig. 2(d)]. Simulations with $r=r(v)$ give results in agreement with the experiments: At constant external driving, the pressure in both Figs. 2(a) and 2(b) passes through a maximum for a critical value of n roughly corresponding to one particle layer. For $n < 1$, most particles are in vertical ballistic motion between the piston and the lid. Thus, the mean pressure increases roughly proportionally to n . When n is increased such that $n > 1$, interparticle collisions become more frequent. The energy dissipation is increased and thus the pressure decreases. This maximum pressure is not due to gravity because it also appears in simulations with $g=0$ and r

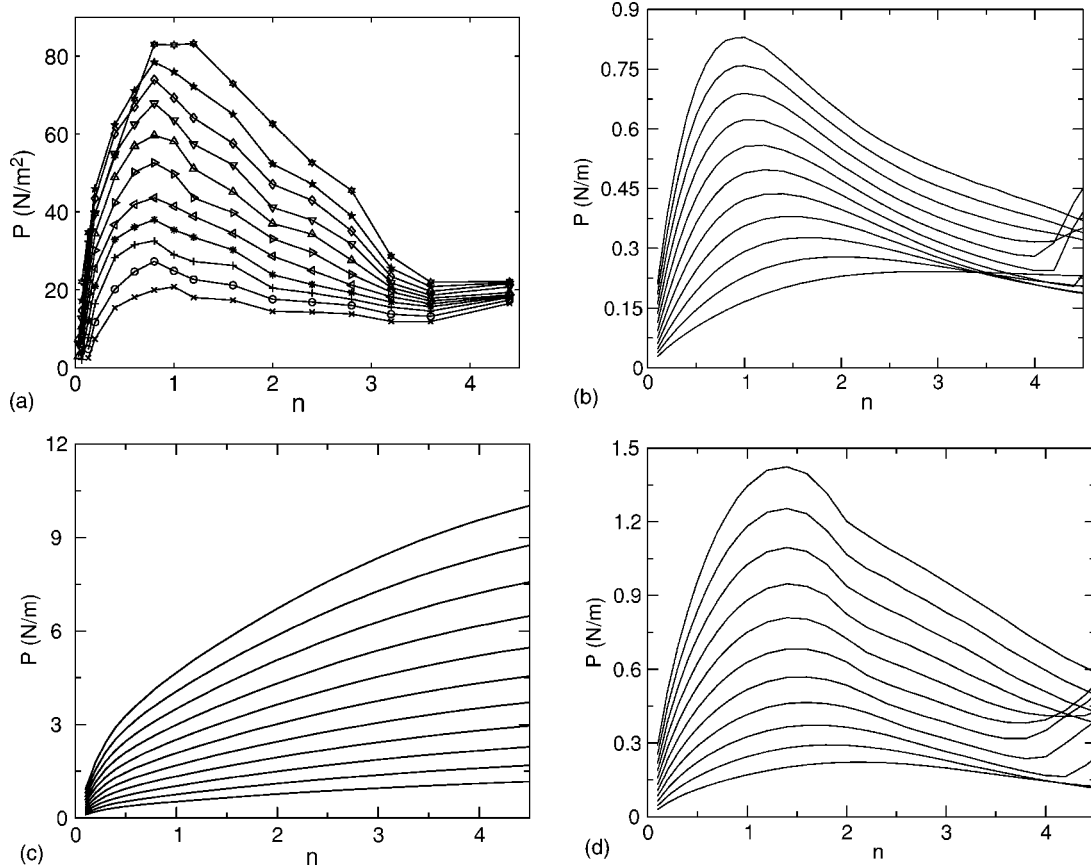


FIG. 2. Time averaged pressure P on the top of the cell as a function of particle layer n for various vibration frequencies f . (a) Experimental results from [10] for stainless steel beads 2 mm in diameter, with $A=25$ mm, $10 \leq f \leq 20$ Hz with a 1 Hz step (from bottom to top) and $h-h_0=5$ mm. (b) Numerical simulation where the coefficient of restitution $r(v)$ is given by Eq. (1). (c) Numerical simulation with a coefficient of restitution of 0.95, independent of impact velocity. (d) Numerical simulation with a coefficient of restitution of 0.7, independent of impact velocity. The simulations (b), (c), and (d) are 2D with gravity, done for 2 mm disks, with $A=25$ mm, $10 \leq f \leq 30$ Hz with a 2 Hz step (from bottom to top) and $h-h_0=15$ mm. In the simulations, the two-dimensional pressure is given in N/m.

$=r(v)$. Furthermore, the maximum persists when g is increased above 9.8 m/s^2 . For $n \geq 4$ and for certain frequencies, a resonance appears in Fig. 2(b) which is controlled by the ratio between the vibration period and the particle flight time under gravity, $\sqrt{g}/h/f$. Turning our attention to Fig. 2(c), we see that setting $r=0.95$ independently of impact velocity gives pressure qualitatively different from experiments. The difference between Figs. 2(b) and 2(c) can be understood by considering a high velocity collision (e.g., $v=1 \text{ m/s}$). In Fig. 2(b), this collision has a restitution coefficient of $r=r(1 \text{ m/s}) \approx 0.7$ (see Fig. 1), whereas in Fig. 2(c), r is fixed at 0.95 for all collisions. This means that for equal collision frequencies, dissipation is much stronger for $r=r(v)$ than for $r=0.95$, because the high velocity collisions dominate the dissipation. Stronger dissipation leads to lower granular temperatures and thus to lower pressures.

We can check this interpretation by changing the constant restitution coefficient to $r=0.7$ and then comparing it to $r=r(v)$. In these two cases, the high velocity collisions will have roughly the same restitution coefficient. We indeed observed a pressure that decreases for large n for constant $r=0.7$ [see Fig. 2(d)]. Therefore, surprisingly, constant $r=0.7$ reproduces more precisely the experimental pressure mea-

surements than constant $r=0.95$, even though $r=0.95$ or 0.9 is often given as the restitution coefficient of steel. However, if we look at other properties, we see that $r=0.7$ and $r=r(v)$ give very different predictions.

For example, in Fig. 3, we show two snapshots from two different simulations one with $r=r(v)$ and another with $r=0.7$, both with $n=3$ in the presence of gravity. When $r=r(v)$, the particles are concentrated in the upper half of the chamber, but they are evenly spread in the horizontal direction [see Fig. 3(a)]. The system is hotter and less dense near the vibrating wall, and colder and denser by the opposite wall. But, when $r=0.7$, the majority of the particles are confined to a tight cluster, pressed against the upper wall, coexisting with low density regions [see Fig. 3(b)]. This instability has already been reported numerically [26], although for much different parameters (constant restitution coefficient $r=0.96$, thermal walls, no gravity, and large n). However, nothing like this was seen experimentally. Therefore, if one is seeking information about particle positions, $r=0.7$ gives incorrect results even though it gives acceptable results for the pressure. We conclude, therefore, that the only way to successfully describe all the properties in all situations is to use a velocity-dependent restitution coefficient model.

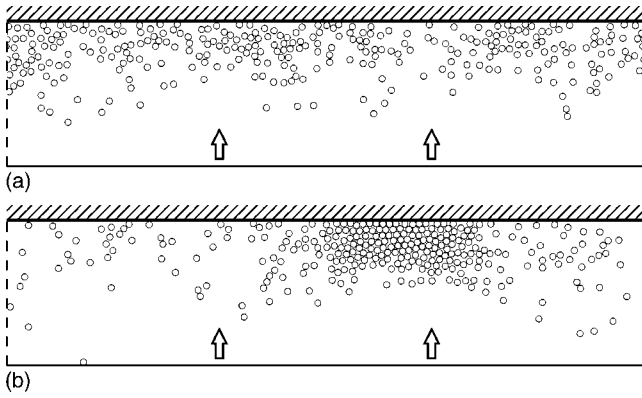


FIG. 3. Snapshots from the simulations with $n=3$, gravity $g \neq 0$, driving frequency $f=30$ Hz, and $h-h_0=15$ mm. The upper wall is stationary, and the lower wall is the piston, which is at its lowest position in both snapshots. The horizontal boundaries are periodic (indicated by dashed lines). Gravity points downward. (a) $r=r(v)$, as given in Eq. (1), and (b) constant $r=0.7$. In (b) we see a tight cluster which was not observed in the experiments.

B. The importance of the particle number

Many authors have postulated that the pressure on the upper wall P (or granular temperature T) is related to the piston velocity V through $P, T \propto V^\theta$. However, it is not clear what the correct “scaling exponent” θ should be. This question has been addressed several times in the past, without a clear resolution of the question [5–8]. For example, kinetic theory [1,7] and hydrodynamic models [8] predict $T \propto V^2$ whereas numerical simulations [3,4] or experiments [1–3] give $T \propto V^\theta$, with $1 \leq \theta \leq 2$. These studies were done at single values of n . In this section, we show that it is very important to explicitly consider the dependence of the scaling exponents on n . We also consider the effect of gravity and a variable coefficient of restitution. Doing so enables us to explain and unify all previous works.

At the upper wall, we measured numerically the collision frequency N_c and the mean impulsion per collision ΔI for various frequencies of the vibrating wall and numbers of particles in the box, with $r=r(v)$ or with $r=0.95$, in the presence or absence of gravity. The time averaged pressure on the upper wall can be calculated from these quantities using

$$P = N_c \Delta I / L. \quad (2)$$

(By conservation of momentum, the time averaged pressure on the lower wall is just P plus the weight of the particles Nmg/L .) The total kinetic energy of the system is also measured to have access to the granular temperature, T . N_c , ΔI , P , and T are all found to fit with power laws in V^θ for our range of piston velocities. Figure 4 shows θ exponents of N_c , ΔI , P , and T as a function of n . When $g=0$ and r is constant [see Fig. 4(a)], we have $P \sim V^2$, $\Delta I \sim V$, and $N_c \sim V$ for all n . We call these relations the classical kinetic theory scaling. This scaling can be established by simple dimensional analysis when the vibration velocity V provides the only time scale in the system. This is the case for $g=0$ and r independent of velocity. However, in the experiments, two additional time scales are provided, one by gravity and the other by the

velocity-dependent restitution coefficient. Numerical simulations can separate the effects of these two time scales on the scaling exponents θ . This is done in Fig. 4(b) [where $g=0$ but $r=r(v)$] and Fig. 4(c) [where r is constant but $g \neq 0$]. In both figures, all the exponents become functions of n . However, the time scale linked to $r=r(v)$ leads to much more dramatic departure from the classical scaling. After considering the two time scales separately, let us consider the case corresponding to most experiments, where both gravity and $r=r(v)$ are present [see Fig. 4(d)]. The similarity between this figure and Fig. 4(b) confirms that the velocity-dependent restitution coefficient has a more important effect than the gravity. Furthermore, only the variation of the restitution coefficient with the particle velocity explains the experiment performed in low gravity [11]. This experiment gives a $V^{3/2}$ pressure scaling [● symbol on Fig. 4(b)] for $n=1$ and a motionless clustered state for $n > 2$. Only the simulation with $r=r(v)$ can reproduce these results [see Fig. 4(b)] whereas constant r simulations leads to the classical scaling [$P \propto V^2$, see Fig. 4(a)] and only a gaseous state for all n shown in the figure.

As shown in Fig. 4, it is thus very important to explicitly consider the dependence of θ on n . In all cases, except the unrealistic case of Fig. 4(a), θ depends on n . To our knowledge, the only experiment [10] to systematically investigate this effect shows that $T \propto V^{\theta(n)}$, with θ continuously varying from $\theta=2$ when $n \rightarrow 0$, as expected from kinetic theory, to $\theta \approx 0$ for large n due to the clustering instability. These experiments [10] performed under gravity (shown in Fig. 5) are well reproduced by the simulations of Fig. 4(d). In both cases, the observed pressure and granular temperature scaling exponents strongly decrease with increasing n .

We finish this section by noting two curious facts about Fig. 4. First of all, in Fig. 4(b) [$g=0$ and $r=r(v)$], $\theta \approx 1$ for the pressure and temperature when $n > 2$. This is the sign of a different robust scaling regime where P and $T \propto V^1$, which will be the topic of a future paper. Second, in Fig. 4(d) [$g \neq 0$ and $r=r(v)$], the scaling exponents are not shown for $n \geq 3$, because the dependence of P , T , N_c , and ΔI on V is no longer a simple power law. (More precisely, we do not plot a point on Fig. 4 when $|\ln(X_{\text{observed}}) - \ln(X_{\text{fitted}})| \geq 0.25$ for any of the 11 simulations used to calculate the exponent—see caption.) The power law breaks down because there is a resonance between the time of flight of the cluster under gravity and the vibration period.

C. The influence of other parameters

In this section, we review the influence of the other simulation parameters (box size, particle rotations, gravity, and the vibration parameters), and show that it is not possible to reproduce the experimental curves in Fig. 2(a) unless one sets $r=r(v)$ or $r=0.7$.

Performing simulations for $5 \leq h-h_0 \leq 50$ mm shows that the shapes of the curves P vs n in Figs. 2(b) and 2(c) remain the same. For $r=r(v)$ [Fig. 2(b)] increasing $h-h_0$ shifts the maximum toward smaller values of n and decreases in amplitude. The only exception occurs when the box height approaches the particle diameter, i.e., $h-h_0=5$ mm, where the

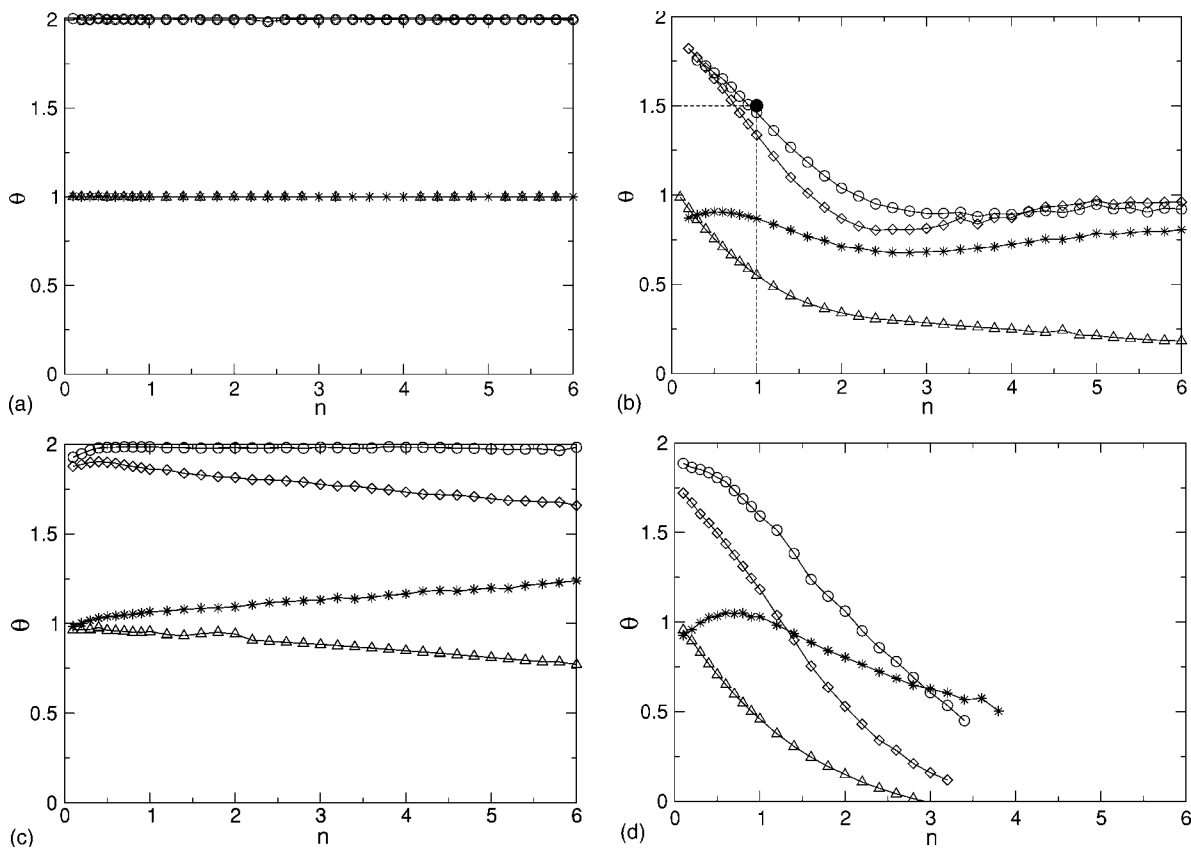


FIG. 4. The exponents θ as a function of n which give the scaling of the granular temperature T (\diamond), collision frequency N_c ($*$), mean impulse ΔI (\triangle), and pressure P (\circ). All these quantities are proportional to $V^{\theta(n)}$. Without gravity, (a) for $r=0.95$ and (b) for $r=r(v)$. With gravity, (c) for $r=0.95$ and (d) for $r=r(v)$. The exponents are obtained by fixing n and performing 11 simulations, varying f from 10 to 30 Hz. Then $\ln(X)$ (where X is the quantity being considered) is plotted against $\ln(V)$. The resulting curve is always nearly a straight line [except for $n > 3$ in (d)—see text], and the exponent is calculated from a least squares fit. The pressure scaling point (\bullet) on (b) is from the experiment [11] performed in low gravity. See Fig. 3(a) for typical snapshot corresponding to $n=3$, $g \neq 0$ and $r=r(v)$.

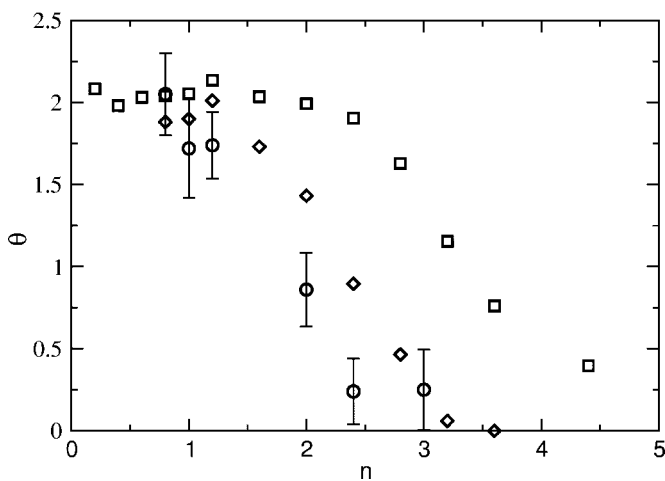


FIG. 5. Experimental data performed under gravity from Ref. [10]: The exponents $\theta(n)$ of time averaged pressure (\square) [see Fig. 2(a)], and kinetic energy extracted from density profile (\circ) or volume expansion (\diamond) measurements. These data should be compared with the simulations of Fig. 4(d).

maximum disappears. Considering $r=0.95$ leads to similar conclusions.

To eliminate the possibility that the experimental curve can be reproduced by taking into account particle rotations, we performed simulations with $r=0.95$ and various values of the tangential restitution coefficient r_t . This parameter is defined as the ratio between the tangential components of the pre- and postcollision relative velocities. Perfectly smooth spheres correspond to $r_t=-1$. When $r_t=1$, the tangential relative velocity is reversed by the collision. These two values $|r_t|=1$ correspond to energy conservation. Energy is dissipated for $-1 < r_t < 1$, $r_t=0$ corresponding to maximum energy dissipation. When $|r_t|$ is close to 1, the P vs n curves are almost unchanged. When r_t is close to 0, the curves become nearly flat for $n > 2$.

Throughout this paper, we have used the piston vibration velocity V to characterize the vibration. It is important to point out that V is not the only way to do this. One could also use the maximum piston acceleration Γ . When Γ is close to g , it controls the behavior of the system, i.e., adjusting A and f while keeping Γ constant does not change the system's

behavior much. But in the simulations presented here, $\Gamma \gg g$, and the system's behavior is controlled by V . This can be checked by multiplying the frequency by 10 while dividing A by 10, thus keeping V the same (while Γ increases by an order of magnitude). Doing so changes the pressure only by about 20%. Therefore, V is the correct parameter to describe the vibration for the simulations considered here.

IV. CONCLUSIONS

In this paper, we brought simulations of a strongly vibrated granular medium as close as possible to the experiments. We showed that the use of a velocity-dependent coefficient of restitution reproduces results that agree with experiments. It is especially important to take into account plastic deformations that cause the restitution coefficient to decrease rapidly with increasing impact velocity. Indeed, the restitution coefficient for strongly vibrated steel spheres is

very far from the constant values of $r=0.95$ or 0.9 that are often cited in simulations as typical for steel spheres. Changing the box size or the gravitational acceleration and including particle rotation do not modify this conclusion. We also noted that it is very important to take into account the number of particle layers n . The dependence of the pressure P on the piston velocity V changes with n . It is not accurate to speak of “a” scaling exponent for the pressure in terms of V : this exponent depends continuously on n , and does not exist at high density ($n > 3$) under gravity, due to the clustering instability.

ACKNOWLEDGMENTS

We thank Stéphan Fauve for fruitful discussions. The authors gratefully acknowledge the hospitality of the ENS-Lyon physics department, which made this collaboration possible.

-
- [1] S. Warr, J. M. Huntley, and G. T. H. Jacques, *Phys. Rev. E* **52**, 5583 (1995).
- [2] X. Yang and D. Candela, *Phys. Rev. Lett.* **85**, 298 (2000); R. D. Wildman, J. M. Huntley, and D. J. Parker, *Phys. Rev. E* **63**, 061311 (2001).
- [3] S. Luding *et al.*, *Phys. Rev. E* **49**, 1634 (1994).
- [4] S. Luding, H. J. Herrmann, and A. Blumen, *Phys. Rev. E* **50**, 3100 (1994); S. Luding, *ibid.* **52**, 4442 (1995); H. J. Herrmann and S. Luding, *Continuum Mech. Thermodyn.* **10**, 189 (1998).
- [5] S. McNamara and S. Luding, *Phys. Rev. E* **58**, 813 (1998).
- [6] J. M. Huntley, *Phys. Rev. E* **58**, 5168 (1998).
- [7] V. Kumaran, *Phys. Rev. E* **57**, 5660 (1998).
- [8] J. Lee, *Physica A* **219**, 305 (1995).
- [9] *Granular Gases*, edited by T. Pöschel and S. Luding, *Lectures Notes in Physics Vol. 564* (Springer-Verlag, Berlin, 2001).
- [10] E. Falcon, S. Fauve, and C. Laroche, in *Granular Gases* (Ref. [9]), pp. 244–253; E. Falcon, S. Fauve, and C. Laroche, *Eur. Phys. J. B* **9**, 183 (1999); *J. Chim. Phys.* **96**, 1111 (1999).
- [11] E. Falcon *et al.*, *Phys. Rev. Lett.* **83**, 440 (1999).
- [12] N. V. Brilliantov and T. Pöschel, *Phys. Rev. E* **61**, 5573 (2000); S. J. Moon, J. B. Swift, and H. L. Swinney, *ibid.* **69**, 011301 (2004).
- [13] C. V. Raman, *Phys. Rev.* **12**, 442 (1918); D. Tabor, *Proc. R. Soc. London, Ser. A* **192**, 247 (1948); W. Goldsmith, *Impact* (Arnold, London, 1960).
- [14] K. L. Johnson, *Contact Mechanics* (Cambridge University Press, Cambridge, U.K., 1985).
- [15] L. Labous, A. D. Rosato, and R. N. Dave, *Phys. Rev. E* **56**, 5717 (1997).
- [16] G. Kuwabara and K. Kono, *Jpn. J. Appl. Phys., Part 1* **26**, 1230 (1987).
- [17] E. Falcon, C. Laroche, S. Fauve, and C. Coste, *Eur. Phys. J. B* **3**, 45 (1998); see also references therein.
- [18] J.-M. Hertzsch, F. Spahn, and N. V. Brilliantov, *J. Phys. II* **5**, 1725 (1995); J. Schäfer, S. Dippel, and D. E. Wolf, *J. Phys. I* **6**, 5 (1996); S. Luding *et al.*, *Phys. Rev. E* **50**, 4113 (1994).
- [19] C. Salueña, T. Pöschel, and S. E. Esipov, *Phys. Rev. E* **59**, 4422 (1999).
- [20] C. Bizon *et al.*, *Phys. Rev. Lett.* **80**, 57 (1998).
- [21] T. Pöschel and N. V. Brilliantov, *Phys. Rev. E* **63**, 021505 (2001).
- [22] D. Goldman *et al.*, *Phys. Rev. E* **57**, 4831 (1998).
- [23] H. Salo, J. Lukkari, and J. Hänninen, *Earth, Moon, Planets* **43**, 33 (1988); F. Spahn, U. Schwarz, and J. Kurths, *Phys. Rev. Lett.* **78**, 1596 (1997); H. Salo, in *Granular Gases* (Ref. [9]) pp. 330–349.
- [24] F. G. Bridges, A. Hatzes, and D. N. C. Lin, *Nature (London)* **309**, 333 (1984); A. Hatzes, F. G. Bridges, and D. N. C. Lin, *Mon. Not. R. Astron. Soc.* **231**, 1091 (1988); K. D. Supulver, F. G. Bridges, and D. N. C. Lin, *Icarus* **113**, 188 (1995); M. Higa, M. Arakawa, and N. Maeno, *Planet. Space Sci.* **44**, 917 (1996).
- [25] J. M. Lifshitz and H. Kolsky, *J. Mech. Phys. Solids* **12**, 35 (1964).
- [26] M. Argentina, M. G. Clerc, and R. Soto, *Phys. Rev. Lett.* **89**, 044301 (2002).